Concentration-Dependent Chemical Expansion in Lithium-Ion Battery Cathode Particles

Veruska Malavé
Department of Mechanical Engineering,
Colorado School of Mines,
Golden, CO 80401
e-mail: vmalaved@mines.edu

J. R. Berger[1]
Department of Mechanical Engineering,
Colorado School of Mines,
Golden, CO 80401
e-mail: jberger@mines.edu

P. A. Martin
Department of Applied Mathematics
and Statistics,
Colorado School of Mines,
Golden, CO 80401
e-mail: pamartin@mines.edu

In this work, the effect of the concentration-dependent chemical-expansion coefficient, β, on the chemo-elastic field in lithium-ion cathode particles is examined. To accomplish this, an isotropic linear-elastic model is developed for a single idealistic particle subjected to potentiostatic-discharge and charge conditions. It is shown that β can be a key parameter in demarcating the chemo-stress–strain state of the cathode material undergoing nonlinear volumetric strains. As an example, such strains develop in the hexagonal-to-monoclinic-phase region of Li_xCoO_2 ($0.37 \le x \le 0.55$) and, subsequently, the corresponding β is a linear function of concentration. Previous studies have assumed a constant value for β. Findings suggest that the composition-generated chemo-elastic field that is based on a linear-β dramatically affects both the interdiffusion and the mechanical behavior of the Li_xCoO_2 cathode particle. Because the chemo-elastic phenomena emanate in a reciprocal fashion, the resulting linear β-based hydrostatic-stress gradients significantly aid the diffusion of lithium. Thus, diffusion is accelerated in either electrochemical process that the cathode material undergoes. [DOI: 10.1115/1.4027833]

1 Introduction

The use of lithium (Li) ion batteries (LIBs) has been extensively investigated in response to increasing high demands for environmentally friendly portable renewable energy devices. Diffusion-induced stresses (DIS) can develop in the electrode particles as a result of compositional inhomogeneities [1]. These stresses are of great concern since the material can undergo significant volume changes under Li intercalation/deintercalation into/out of the host material. The accumulated structural changes can enhance proneness to particle fracture [1]. The phenomena of DIS and correlated stress-induced diffusion (SID) have been investigated based on the thermodynamics of stressed solids; more specifically, under the delineation of a modified chemical-potential concept. In the classical Fickian diffusion, which has been typically used in electrochemistry-related studies of LIB electrodes, the contribution of the elastic energy induced by the diffusing substance is neglected. The composition gradients that emerge inside the particle can be affected by elastic self-stresses, which arise from the nonuniform solute-composition distribution, and such an effect cannot be captured by the classical Fickian relation. One of the first theories to formulate an expression of the chemical potential in interdiffusion analyses of a multicomponent stressed solid was developed by Larché and Cahn [2]. Bohn et al. [3] proposed a nonideal chemical-potential relation, μ, for LIB electrodes where the parameter g was introduced to account for the Li–ion interaction within the solid material, neglecting the dependence of elastic constants on solute composition, C. The chemical potential was taken as

$$\mu = \mu_0 + gRT\frac{C}{C_{\max}} + RT\log\left(\frac{C}{C_{\max}-C}\right) - \Omega\sigma_{\mathrm{h}} \tag{1}$$

where μ_0 is a constant, R is the gas constant, T is the temperature, Ω is the partial molar volume, σ_{h} is the hydrostatic stress, and $C_{\max}$ represents the stoichiometric solute concentration in the host lattice. It can be inferred that the parameter g in Eq. (1) is only applicable to solid electrode materials in which ionic diffusion occurs and/or the analysis is oriented to the electrode–electrolyte interface.

A few authors have investigated the contribution of concentration-dependent elastic constants [4–10] and concentration-dependent effective diffusivity [7,8,11,12] in the Li flux and resulting LIB electrode stress-state. Regarding the former, Yang et al. [8] and He et al. [10] used a linear Li-content-dependent Young's modulus in Si and Si–graphite, respectively. In their work [8,10], the Larché–Cahn chemical-potential approach [2] for a binary-alloy solid solution was employed. He et al. [10] expressed their modification of Eq. (1) as

$$\mu = \mu_0 + RT\log\left(\frac{C}{C_{\max}-C}\right) - \Omega\sigma_{\mathrm{h}} - \frac{\partial}{\partial C}\left(\frac{1-\nu}{E}\right)\sigma_{\mathrm{h}}^2 \tag{2}$$

which satisfies the non-Fickian conservation of species relation

$$\frac{\partial C}{\partial t} = D\frac{\partial}{\partial z}\left[\left(\frac{C_{\max}}{C_{\max}-C}\right)\frac{\partial C}{\partial z} - \frac{\Omega C}{RT}\frac{\partial \sigma_{\mathrm{h}}}{\partial z} + \frac{(1-\nu)C}{RT}\frac{\partial}{\partial z}\left(\frac{\sigma_{\mathrm{h}}^2}{E^2}\frac{\partial E}{\partial C}\right)\right] \tag{3}$$

assuming one-dimensional diffusion in the z-direction along the axis of the anode structure.

Numerical solutions have been proposed for the analysis of the coefficient of diffusion when this strictly depends on the diffusing-substance concentration [3,13,14]. However, in the case of LIB electrode materials, there is no clear agreement in the literature with respect to whether the Li diffusivity depends only on composition or if the driving force is constituted by the mass-transfer activity gradient [15,16]. In a nonideal Li-flux analysis in electrode materials, Bohn et al. [3] and Purkayastha and McMeeking [14] presented a model wherein a concentration-dependent mobility of the Li, M, is implemented in the flux relation, $\mathbf{J} = -MC\nabla\mu$,

[1]Corresponding author.

Contributed by the Applied Mechanics Division of ASME for publication in the Journal of Applied Mechanics. Manuscript received May 13, 2014; final manuscript received June 5, 2014; accepted manuscript posted June 11, 2014; published online June 23, 2014. Assoc. Editor: Pradeep Sharma.

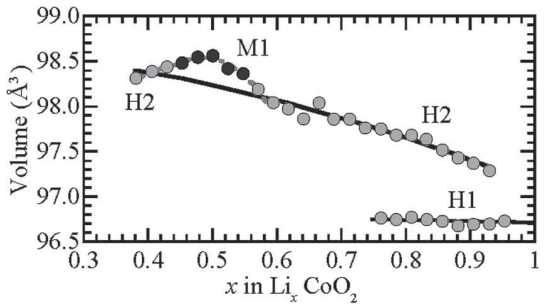

Fig. 1 Li_xCoO_2 crystal volume as a function of Li content (adapted from Reimers and Dahn [28]). The monoclinic phase is labeled as M1; two hexagonal phases are labeled as H1 and H2.

$$M = M_0\left(1 - \frac{C}{C_{\max}}\right) \tag{4}$$

where M_0 is the concentration-independent mobility. A modified version of non-Fickian diffusion relation was then calculated as

$$\mathbf{J} = D_0\left\{\left[1 + \frac{C}{C_{\max}}\left(1 - \frac{C}{C_{\max}}\right)\left(g + C\frac{dg}{dC}\right)\right]\nabla C - \left(1 - \frac{C}{C_{\max}}\right)\frac{\Omega C}{RT}\nabla\sigma_h\right\} \tag{5}$$

The value of Ω has been established as a key parameter influencing the diffusion of Li and stress–strain state in the $Li_xMn_2O_4$ material [14,17]. In the published literature, a vast number of studies oriented to the LIB-electrode mechanical response upon the hydrostatic-stress-gradient contribution [14,18–26] have implemented the modified chemical-potential relation wherein Ω is constant. With the exception of the works of Chung et al. [22] and Lim et al. [26], which were oriented to Li_xCoO_2 cathode particles, the cathode-based material studied was $Li_xMn_2O_4$, wherein the constant-β assumption could be appropriately based on the measured data presented in Ref. [27]. Nevertheless, a number of cathode materials, such as Li_xCoO_2 [28], $Li_{1+x}Fe_{1-x}PO_4$ [29], and Li_xNiO_2 [30], exhibit nonlinear volumetric changes upon variant Li-composition.[2] To the authors' knowledge, however, no formulation addressing how a composition-dependent β (or Ω) affects the chemo-elastic field of LIB electrodes is found in the literature.

In this investigation, an isotropic linear-elastic model is developed to elucidate the effects of a linear concentration-dependent chemical-expansion coefficient, β, on the DIS and correlated SID of Li_xCoO_2 particles. Based on the experimental data provided by Reimers and Dahn [28], illustrated in Fig. 1, the use of a linear β (β_L) is more appropriate during the nonlinear volumetric contraction/expansion in the hexagonal-to-monoclinic (H2-to-M1) phase transition in the Li_xCoO_2 crystal structure ($0.37 \le x \le 0.55$). The Li diffusion and mechanics in the active-electrode material during intercalation and deintercalation is carried out using an idealized spherical particle. The formulation presented here incorporates a composition-variant diffusivity to consider the effect of the lithiation/delithiation state on Li mobility. The elastic constants of the cathode material are considered to be constant throughout the lithiation process. The electrode–electrolyte interaction is modeled through a boundary condition on the particle surface that describes the Li concentration in terms of electrochemical discharge-and-charge potentiostatic conditions (constant potential control).

The present approach and solution formulations can be applied to on-going research in LIB electrodes undergoing nonlinear crystal volume changes during battery operation. Although the examined compositional range may be unrepresentative of the practical compositional Li_xCoO_2 material in commercial batteries ($0.50 \le x \le 1.00$), an improved understanding of the nature of emerging coupled SID-DIS is desirable in the development of this LIB cathode material and potential derivatives. Extensions of the principles proposed in the current work include applications in the thermal sciences to delineate the contribution of temperature-dependent thermal-expansion coefficients in the thermomechanical field.

2 Diffusion With Concentration-Dependent Chemical Expansion

The general case where β (or equivalently Ω) is a function of the solute concentration, C, across an entire concentration range is examined here. The partial molar volume, Ω, where $\Omega = 3\beta$, is determined from the change in the crystal volume, V, with respect to concentration between two concentration values C_1 and C_2 as [19]

$$\Omega = \frac{(\Delta V/V_0)_{1-2}}{\Delta C}$$

where V_0 is the reference volume and $\Delta C = C_2 - C_1$. For cases in which the volume change is linear with respect to composition, β (or Ω) is related to the (constant) slope of the linear $\Delta V/V_0$ curve. If $\Delta V/V_0$ varies quadratically

$$(\Delta V/V_0)_{1-2} = a(\Delta C)^2 + b\Delta C$$

say, then $\Omega(C) = a\Delta C + b$, or in terms of the coefficient of chemical expansion

$$\beta(C) = \xi\Delta C + \eta \tag{6}$$

where $\xi = a/3$ and $\eta = b/3$.

In the mathematical model presented here, the nonclassical chemical potential, μ, is implemented as [2]

$$\mu = \mu_0 + RT\log\left(\frac{C}{C_{\max} - C}\right) - 3\beta\sigma_h \tag{7}$$

Here, β is allowed to be composition-dependent, $\beta = \beta(C)$. Equation (7) is Eq. (1) when $g = 0$. C itself depends on the spatial variable, $\mathbf{x}$; so, derivatives of $\beta(C)$ with respect to x_j are calculated using

$$\frac{\partial\beta}{\partial x_j} = \frac{d\beta}{dC}\frac{\partial C}{\partial x_j}$$

The chemical species flux, $\mathbf{J} = -MC\nabla\mu$, is calculated using Eq. (7),

$$\mathbf{J} = -MRT\left\{\left(\frac{C_{\max}}{C_{\max} - C} - \frac{3\sigma_h C}{RT}\frac{d\beta}{dC}\right)\nabla C - \frac{3\beta C}{RT}\nabla\sigma_h\right\} \tag{8}$$

Note in Eq. (8), the term involving $(d\beta/dC)$. This term will generate additional concentration gradient terms in the final equation for the flux. Under the assumption that M decreases linearly with the Li-composition fraction, the relation in Refs. [3] and [14], Eq. (4), is used giving

$$\mathbf{J} = -D_0\left(1 - \frac{C}{C_{\max}}\right) \times \left\{\left(\frac{C_{\max}}{C_{\max} - C} - \frac{3\sigma_h C}{RT}\frac{d\beta}{dC}\right)\nabla C - \frac{3\beta C}{RT}\nabla\sigma_h\right\} \tag{9}$$

[2]Crystal volumetric variations in other LIB electrode materials, such as $Li_xM_{1/6}Mn_2O_4$ derivative cathodes (M = Cr, Co, and Ni) and Li-alloy anodes, appear to experience linear volume changes with Li content [31,32].

where $D_0 = M_0 RT$. Next, the diffusion of the chemical species is computed from

$$\frac{\partial C}{\partial t} + \nabla \cdot \mathbf{J} = 0 \tag{10}$$

Substituting for $\mathbf{J}$ leads to

$$\begin{aligned}\frac{1}{D_0}\frac{\partial C}{\partial t} = &\left\{1 - \left(1 - \frac{C}{C_{\max}}\right)\alpha\sigma_{\mathrm{h}} C \frac{d\beta}{dC}\right\}\nabla^2 C \\ &- \left(1 - \frac{C}{C_{\max}}\right)\alpha C\beta\nabla^2\sigma_{\mathrm{h}} - \alpha\sigma_{\mathrm{h}}\left\{\left(1 - \frac{2C}{C_{\max}}\right)\frac{d\beta}{dC}\right. \\ &\left. + \left(1 - \frac{C}{C_{\max}}\right)C\frac{d^2\beta}{dC^2}\right\}|\nabla C|^2 - \alpha\left\{\beta\left(1 - \frac{2C}{C_{\max}}\right)\right. \\ &\left. + \left(1 - \frac{C}{C_{\max}}\right)\left(2C\frac{d\beta}{dC}\right)\right\}(\nabla C)\cdot(\nabla\sigma_{\mathrm{h}})\end{aligned} \tag{11}$$

where $\alpha = 3/(RT)$. When β is constant, Eq. (11) reduces to

$$\begin{aligned}\frac{1}{D_0}\frac{\partial C}{\partial t} = &\nabla^2 C - \left(1 - \frac{C}{C_{\max}}\right)\alpha C\beta\nabla^2\sigma_{\mathrm{h}} \\ &- \alpha\beta\left(1 - \frac{2C}{C_{\max}}\right)(\nabla C)\cdot(\nabla\sigma_{\mathrm{h}})\end{aligned} \tag{12}$$

This agrees with Ref. [14], Eq. (39(*b*)). When $\beta = 0$, the standard linear diffusion equation for C is recovered.

For cases in which a constant mobility is assumed, $M = M_0$, Eq. (10) gives

$$\begin{aligned}\frac{1}{D_0}\frac{\partial C}{\partial t} = &\left(\frac{C_{\max}}{C_{\max} - C} - \alpha\sigma_{\mathrm{h}} C\frac{d\beta}{dC}\right)\nabla^2 C - \alpha C\beta\nabla^2\sigma_{\mathrm{h}} \\ &+ \left(\frac{C_{\max}}{(C_{\max} - C)^2} - \alpha\sigma_{\mathrm{h}}\frac{d\beta}{dC} - \alpha\sigma_{\mathrm{h}} C\frac{d^2\beta}{dC^2}\right)|\nabla C|^2 \\ &- \alpha\left(2C\frac{d\beta}{dC} + \beta\right)(\nabla C)\cdot(\nabla\sigma_{\mathrm{h}})\end{aligned} \tag{13}$$

which should be compared with Eq. (11). Note that Eq. (13) does not reduce to the linear diffusion equation when $\beta = 0$. In addition, there is potential singular (nonphysical) behavior as C approaches $C_{\max}$. Thus, Eq. (11) is used.

3 Equilibrium and Constitutive Equation

The mechanical field is treated as quasi-static since the elastic wave speeds are far in excess of the diffusion. In the absence of body forces, the stresses, σ_{ij}, are in equilibrium

$$\frac{\partial\sigma_{ij}}{\partial x_j} = 0, \quad i = 1, 2, 3 \tag{14}$$

The stresses are related to the strains, ε_{ij}, and the concentration, C, by a constitutive relation. For an isotropic solid, the analogous thermoelastic generalization of Hooke's law [33] is used

$$\sigma_{ij} = \lambda\varepsilon_{kk}\delta_{ij} + 2G\varepsilon_{ij} - (3\lambda + 2G)f(C)\delta_{ij} \tag{15}$$

where λ and G are the Lamé moduli, and $f(C)$ is a dimensionless function of C. For a linear relationship between the volume change and concentration, this is

$$f(C) = \beta\Delta C \quad \text{where} \quad \Delta C = C - C_0 \tag{16}$$

and C_0 is the reference concentration at zero strain. In terms of a quadratic relationship between the volume change and concentration this is expressed as

$$f(C) = \xi(\Delta C)^2 + \eta\Delta C \tag{17}$$

or in terms of a linear β

$$f(C) = \beta(C)\Delta C, \quad \beta(C) = \xi\Delta C + \eta \tag{18}$$

From Eq. (15),

$$\sigma_{kk} = (3\lambda + 2G)(\varepsilon_{kk} - 3f) \tag{19}$$

Equilibrium, Eq. (14), gives

$$0 = \frac{\partial\sigma_{ij}}{\partial x_j} = \lambda\frac{\partial\varepsilon_{kk}}{\partial x_i} + 2G\frac{\partial\varepsilon_{ij}}{\partial x_j} - (3\lambda + 2G)\frac{\partial f}{\partial x_i}$$

Differentiating with respect to x_i gives

$$0 = (\lambda + 2G)\nabla^2\varepsilon_{kk} - (3\lambda + 2G)\nabla^2 f$$

after contraction. But, from Eq. (19),

$$3\nabla^2\sigma_{\mathrm{h}} = (3\lambda + 2G)\nabla^2(\varepsilon_{kk} - 3f)$$

Hence, eliminating $\nabla^2\varepsilon_{kk}$ results in

$$3(\lambda + 2G)\nabla^2\sigma_{\mathrm{h}} + 4G(3\lambda + 2G)\nabla^2 f = 0 \tag{20}$$

In terms of Young's modulus, E, and Poisson's ratio, ν, Eq. (20) becomes

$$\nabla^2\sigma_{\mathrm{h}} + \frac{2E}{3(1 - \nu)}\nabla^2 f = 0 \tag{21}$$

This relation, due to Yang [34] when f is a constant multiple of C, is used to simplify Eq. (11) to some degree. It is also employed to simplify the solution for a spherical particle. It is noted that Eq. (21) represents a constraint on the relationship between the hydrostatic stress and the choice for $f(C)$.

4 The Spherical Particle

For a simple example, a spherical particle of radius r_{s} with associated spherically symmetric boundary conditions is considered. These boundary conditions are taken as $\sigma_{rr} = 0$ and $C = C_{\mathrm{s}}$ (a constant value) at $r = r_{\mathrm{s}}$, where r is a spherical polar coordinate. The constant maximum-concentration boundary condition represents a potentiostatic state in a battery cathode. This constant-voltage boundary condition has been commonly used in studies of the stress–strain state of LIB electrode materials [10,17,35–37].

The whole problem involves a coupling between a nonlinear diffusionlike equation and a linear elasticitylike equation. In this section, the linear part of the problem is solved. The main objective is to obtain an explicit relation between the hydrostatic stress, σ_{h}, and the concentration, C. Both of these quantities are functions of r and t (only). Later, the stress components within the particle are required.

4.1 Direct Solution. In spherical coordinates (r, θ, ϕ), the problem depends only on the radial coordinate, r. The corresponding displacement components are $u_r = u(r)$ and $u_\theta = u_\phi = 0$ [38]. The displacement equilibrium equations for spherically symmetric problems reduce to [33]

$$\frac{d}{dr}\left(\frac{du}{dr} + \frac{2u}{r}\right) = \frac{1 + \nu}{1 - \nu}\frac{df}{dr} \tag{22}$$

where f is a specified function of C; refer to Eq. (16). Note that, in this section, C and u are denoted as functions of r only; the dependence on t plays no role.

The solution of Eq. (22) in the thermoelastic case, with constant coefficient of thermal expansion ($f(T) = \alpha\Delta T$), has been presented in Ref. [38]. In the situation reported here, a slightly modified solution is presented as

$$\sigma_{rr} = \frac{2E}{1-\nu}\left(\frac{1}{r_s^3}\int_0^{r_s} f\rho^2 d\rho - \frac{1}{r^3}\int_0^{r} f\rho^2 d\rho\right) \tag{23}$$

$$\sigma_{\theta\theta} = \sigma_{\phi\phi} = \frac{E}{1-\nu}\left(\frac{2}{r_s^3}\int_0^{r_s} f\rho^2 d\rho + \frac{1}{r^3}\int_0^{r} f\rho^2 d\rho - f\right) \tag{24}$$

These equations reduce to those presented in Ref. [38] for thermoelasticity with constant coefficient of thermal expansion. Note that the individual stress components given by Eqs. (23) and (24) contain two contributions (the two integrals appearing in the stress equations): a contribution dependent on the position r where the stress is to be computed, and a global contribution given by the integral over the entire volume of the spherical particle. Additionally, the stresses given by Eq. (24) contain a local contribution given by the last term.

The hydrostatic stress $\sigma_h = (\sigma_{rr} + \sigma_{\theta\theta} + \sigma_{\phi\phi})/3$ can be computed

$$\sigma_h(r) = \frac{2E}{3(1-\nu)}\left(\frac{3}{r_s^3}\int_0^{r_s} f(C(\rho))\rho^2 d\rho - f(C(r))\right) \tag{25}$$

This agrees with Ref. [19] when $f(C) = \beta\Delta C$ and β is a constant.

4.2 Alternative Method for Calculation of σ_h. For solutions of interest, which involve spherical symmetry, Yang's relation Eq. (21) implies that

$$\sigma_h + \frac{2E}{3(1-\nu)}f = A + \frac{B}{r} \tag{26}$$

where A and B are constants.[3] For solutions bounded at the center of the sphere at $r = 0$, $B = 0$. In order to find the constant A, Eq. (26) is integrated over the particle

$$\frac{4}{3}\pi r_s^3 A = 4\pi\int_0^{r_s}\left(\frac{2Ef}{3(1-\nu)} + \sigma_h\right)r^2 dr$$

Thus,

$$A = \frac{2E}{r_s^3(1-\nu)}\int_0^{r_s} f r^2 dr + \frac{3}{r_s^3}\int_0^{r_s}\sigma_h r^2 dr$$

It will be shown that the second integral vanishes, assuming that the surface of the particle at $r = r_s$ is traction free, $\sigma_{rr}(r_s) = 0$. Then, using Eq. (26), it is found that σ_h is given by Eq. (25), as presented before. To demonstrate that the integral of the hydrostatic stress over the spherical particle vanishes, the radial equilibrium equation is invoked

$$0 = \frac{d\sigma_{rr}}{dr} + \frac{1}{r}(2\sigma_{rr} - \sigma_{\theta\theta} - \sigma_{\phi\phi}) = \frac{d\sigma_{rr}}{dr} + \frac{1}{r}(3\sigma_{rr} - 3\sigma_h)$$

Hence,

$$3\sigma_h r^2 = r^3\frac{d\sigma_{rr}}{dr} + 3r^2\sigma_{rr} = \frac{d}{dr}(r^3\sigma_{rr})$$

Finally, integrate and use the traction-free boundary condition at $r = r_s$. It is remarked that

$$\int_{\text{particle}}\sigma_h dV = 0 \tag{27}$$

even though the stress components are not all zero.

5 The Spherical Particle: Tentative Scaling

In the idealized-particle problem, the equations are made dimensionless by appropriate scaling. This is to allow the approach of the current work to be applicable in the study of any LIB electrode material. Thus,

$$\hat{C} = \frac{C}{C_{\max}}, \quad \hat{\sigma}_h = \frac{\gamma}{E}\sigma_h, \quad \hat{\beta}(\hat{C}) = \frac{3E}{\gamma RT}\beta(C) \tag{28}$$

where γ is a dimensionless constant to be selected later and $\hat{\beta}$ is a dimensionless function of $\hat{C}$. The first two terms (left to right) in Eq. (28) are dimensionless variables used in related works [17,19]. The dimensionless $\hat{\beta}$ (third relation in Eq. (28)) has been reformulated in this study so that this parameter is composition-dependent. Equation (11) becomes

$$\begin{aligned}\frac{1}{D_0}\frac{\partial\hat{C}}{\partial t} = {} & \left\{1 - (1-\hat{C})\hat{\sigma}_h\hat{C}\frac{d\hat{\beta}}{d\hat{C}}\right\}\nabla^2\hat{C} - (1-\hat{C})\hat{C}\hat{\beta}\nabla^2\hat{\sigma}_h \\ & - \hat{\sigma}_h\left\{(1-2\hat{C})\frac{d\hat{\beta}}{d\hat{C}} + (1-\hat{C})\hat{C}\frac{d^2\hat{\beta}}{d\hat{C}^2}\right\}\left|\nabla\hat{C}\right|^2 \\ & - \left\{\hat{\beta}(1-2\hat{C}) + 2\hat{C}(1-\hat{C})\frac{d\hat{\beta}}{d\hat{C}}\right\}\nabla\hat{C}\cdot\nabla\hat{\sigma}_h\end{aligned} \tag{29}$$

If f is defined by Eq. (18), it is found that

$$f(C) = \frac{1}{3}\gamma\mathcal{R}(\hat{C} - \hat{C}_0)\hat{\beta}(\hat{C}) \tag{30}$$

with $\hat{C}_0 = C_0/C_{\max}$ and $\mathcal{R} = RTC_{\max}/E$. The quantity $\mathcal{R}$ is a dimensionless number. Numerical values in Ref. [14] for $Li_xMn_2O_4$ give $\mathcal{R} \simeq 0.00057$; for Li_xCoO_2, $\mathcal{R} \simeq 0.00015$. The Yang relation, Eq. (21), becomes

$$\nabla^2\hat{\sigma}_h + \frac{2\gamma^2\mathcal{R}}{9(1-\nu)}\nabla^2\left\{(\hat{C} - \hat{C}_0)\hat{\beta}(\hat{C})\right\} = 0 \tag{31}$$

For the symmetric spherical particle studied here, $\hat{\sigma}_h$ is given by Eq. (25), whence

$$\hat{\sigma}_h(r) = \frac{2\gamma^2\mathcal{R}}{9(1-\nu)}\left\{\frac{3}{r_s^3}\int_0^{r_s}(\hat{C} - \hat{C}_0)\hat{\beta}\rho^2 d\rho - (\hat{C} - \hat{C}_0)\hat{\beta}\right\} \tag{32}$$

To simplify Eqs. (31) and (32), γ is chosen so that the common prefactor equals 1,

$$\gamma = \sqrt{\frac{9(1-\nu)}{2\mathcal{R}}} = \sqrt{\frac{9(1-\nu)E}{2RTC_{\max}}} \tag{33}$$

For Li_xCoO_2, $\gamma \simeq 150$.

6 Quadratic Volume Change

As a specific example, consider the isotropic case of the spherical particle where the volume change is quadratic with respect to concentration. From Eqs. (18) and (28)

$$\hat{\beta}(\hat{C}) = \hat{\xi}\Delta\hat{C} + \hat{\eta}$$

[3]The general spherically symmetric solution of Laplace's equation, $\nabla^2\Phi = 0$, is $\Phi(r) = A + B/r$.

where

$$\hat{\xi} = \frac{3E}{\gamma RT} C_{\max} \xi, \quad \hat{\eta} = \frac{3E}{\gamma RT} \eta$$

In order to scale our numerical solution, let

$$\hat{r} = r/r_s, \quad \hat{t} = tD_0/r_s^2$$

Now write Eq. (32) with γ chosen as in Eq. (33)

$$\hat{\sigma}_h = \hat{\mathcal{I}} - (\hat{\xi}\Delta\hat{C} + \hat{\eta})\Delta\hat{C} \tag{34}$$

where

$$\hat{\mathcal{I}} = 3\int_0^1 (\hat{\xi}\Delta\hat{C} + \hat{\eta})\Delta\hat{C}\hat{\rho}^2 d\hat{\rho}.$$

Note that $\hat{\mathcal{I}}$ will be spatially constant at a given time step. The normalized derivatives are then

$$\frac{\partial\hat{\sigma}_h}{\partial\hat{r}} = -\frac{\partial\hat{C}}{\partial\hat{r}}\left(2\hat{\xi}\Delta\hat{C} + \hat{\eta}\right) \tag{35}$$

and

$$\frac{\partial^2\hat{\sigma}_h}{\partial\hat{r}^2} = -\frac{\partial^2\hat{C}}{\partial\hat{r}^2}\left(2\hat{\xi}\Delta\hat{C} + \hat{\eta}\right) - 2\hat{\xi}\left(\frac{\partial\hat{C}}{\partial\hat{r}}\right)^2 \tag{36}$$

Equation (29) becomes

$$\begin{aligned}\frac{\partial\hat{C}}{\partial\hat{t}} = &\left\{1 - (1-\hat{C})(\hat{\mathcal{I}} - (\hat{\xi}\Delta\hat{C} + \hat{\eta})\Delta\hat{C})\hat{C}\hat{\xi}\right\}\nabla^2\hat{C} \\ &- (1-\hat{C})\hat{C}(\hat{\xi}\Delta\hat{C} + \hat{\eta})\nabla^2\hat{\sigma}_h \\ &- (\hat{\mathcal{I}} - (\hat{\xi}\Delta\hat{C} + \hat{\eta})\Delta\hat{C})\left\{(1-2\hat{C})\hat{\xi}\right\}|\nabla\hat{C}|^2 \\ &- \left\{(\hat{\xi}\Delta\hat{C} + \hat{\eta})(1-2\hat{C}) + 2\hat{C}(1-\hat{C})\hat{\xi}\right\}\nabla\hat{C}\cdot\nabla\hat{\sigma}_h\end{aligned} \tag{37}$$

In the special case of full spherical symmetry, Eq. (37) is

$$\begin{aligned}\frac{\partial\hat{C}}{\partial\hat{t}} = &\left\{1 - (1-\hat{C})\left[\hat{\mathcal{I}} - (\hat{\xi}\Delta\hat{C} + \hat{\eta})\Delta\hat{C}\right]\hat{C}\hat{\xi}\right\}\left(\frac{\partial^2\hat{C}}{\partial\hat{r}^2} + \frac{2}{\hat{r}}\frac{\partial\hat{C}}{\partial\hat{r}}\right) \\ &- (1-\hat{C})\hat{C}(\hat{\xi}\Delta\hat{C} + \hat{\eta})\left(\frac{\partial^2\hat{\sigma}_h}{\partial\hat{r}^2} + \frac{2}{\hat{r}}\frac{\partial\hat{\sigma}_h}{\partial\hat{r}}\right) \\ &- \left[\hat{\mathcal{I}} - (\hat{\xi}\Delta\hat{C} + \hat{\eta})\Delta\hat{C}\right]\left\{(1-2\hat{C})\hat{\xi}\right\}\left(\frac{\partial\hat{C}}{\partial\hat{r}}\right)^2 \\ &- \left\{(\hat{\xi}\Delta\hat{C} + \hat{\eta})(1-2\hat{C}) + 2\hat{C}(1-\hat{C})\hat{\xi}\right\}\frac{\partial\hat{C}}{\partial\hat{r}}\frac{\partial\hat{\sigma}_h}{\partial\hat{r}}\end{aligned} \tag{38}$$

Finally, using Eqs. (35) and (36), Eq. (38) becomes

$$\frac{\partial\hat{C}}{\partial\hat{t}} = \left(\frac{\partial^2\hat{C}}{\partial\hat{r}^2} + \frac{2}{\hat{r}}\frac{\partial\hat{C}}{\partial\hat{r}}\right)A_1(\hat{C}) + \left(\frac{\partial\hat{C}}{\partial\hat{r}}\right)^2 A_2(\hat{C}) \tag{39}$$

where

$$\begin{aligned}A_1(\hat{C}) = &1 - (1-\hat{C})\left[\hat{\mathcal{I}} - (\hat{\xi}\Delta\hat{C} + \hat{\eta})\Delta\hat{C}\right]\hat{C}\hat{\xi} \\ &+ (1-\hat{C})\hat{C}(\hat{\xi}\Delta\hat{C} + \hat{\eta})(2\hat{\xi}\Delta\hat{C} + \hat{\eta})\end{aligned} \tag{40}$$

$$\begin{aligned}A_2(\hat{C}) = &-\left[\hat{\mathcal{I}} - (\hat{\xi}\Delta\hat{C} + \hat{\eta})\Delta\hat{C}\right](1-2\hat{C})\hat{\xi} \\ &+ 2\hat{\xi}(1-\hat{C})\hat{C}(\hat{\xi}\Delta\hat{C} + \hat{\eta}) + \left[(\hat{\xi}\Delta\hat{C} + \hat{\eta})(1-2\hat{C})\right. \\ &\left.+ 2\hat{C}(1-\hat{C})\hat{\xi}\right](2\hat{\xi}\Delta\hat{C} + \hat{\eta})\end{aligned} \tag{41}$$

Note that when $\hat{\xi} = \hat{\eta} = 0$, $A_1 = 1$, $A_2 = 0$, and Eq. (39) reduces properly to the classical Fickian diffusion equation (i.e., no mechanical contribution in the solute flux). The initial condition is taken as $\hat{C}(\hat{r}, 0) = \hat{C}_i$, which is the initial concentration of Li in the particle everywhere except on the surface of the sphere. The traction-free boundary condition on the surface of the particle has already been satisfied, so the particle is free to contract/expand. The potentiostatic boundary condition is imposed on the surface of the particle, so that the Li content remains invariant on the surface, $\hat{C}(1, \hat{t}) = \hat{C}_s$.

7 Finite Difference Formulation

For numerical computation, an explicit finite difference method for the diffusion equation, Eq. (39), is formulated. A forward difference representation for the spatial and time derivatives, and the second-order spatial derivative is approximated in the typical way

$$\frac{\partial^2\hat{C}}{\partial\hat{r}^2} \approx \frac{\hat{C}_{i+1,j} - 2\hat{C}_{i,j} + \hat{C}_{i-1,j}}{(\Delta\hat{r})^2}$$

where $\Delta\hat{r}$ is the spatial discretization, $\hat{C}_{i,j} \approx \hat{C}(i\Delta\hat{r}, j\Delta\hat{t})$, and $\Delta\hat{t}$ is the temporal discretization. The difference formula is

$$\begin{aligned}\hat{C}_{i,j+1} = &\hat{C}_{i+1,j}\left\{A_1(\hat{C})s\left(1 + 2\frac{\Delta\hat{r}}{\hat{r}_i}\right) + A_2(\hat{C})s\right\} \\ &+ \hat{C}_{i,j}\left\{1 - A_1(\hat{C})s\left(1 + 2\frac{\Delta\hat{r}}{\hat{r}_i}\right) + A_2(\hat{C})s\right\} \\ &+ \hat{C}_{i-1,j}A_1(\hat{C})s\end{aligned} \tag{42}$$

where $s = \Delta\hat{t}/(\Delta\hat{r})^2$ and $\hat{r}_i = i\Delta\hat{r}$. The repeated trapezoidal rule is used to compute $\hat{\mathcal{I}}$ so the nodal values needed for the concentration are at the same locations as are needed for the finite difference expressions. In this case, noting that the integrand equals zero at $\hat{r} = 0$

$$\hat{\mathcal{I}} \approx 3h\sum_{i=1}^{N-1}\Delta\hat{C}_{i,j}(\hat{\xi}\Delta\hat{C}_{i,j} + \hat{\eta})\hat{r}_i^2 + \frac{3h}{2}\Delta\hat{C}_{N,j}(\hat{\xi}\Delta\hat{C}_{N,j} + \hat{\eta})$$

Finally, note that Eq. (39) cannot be directly evaluated at $\hat{r} = 0$. Following Ref. [39], consider a Maclaurin expansion for $\partial\hat{C}/\partial\hat{r}$

$$\frac{\partial\hat{C}}{\partial\hat{r}}(\hat{r}, \hat{t}) = \frac{\partial\hat{C}}{\partial\hat{r}}(0, \hat{t}) + \hat{r}\frac{\partial^2\hat{C}}{\partial\hat{r}^2}(0, \hat{t}) + \cdots$$

As $\partial\hat{C}/\partial\hat{r} = 0$ at $\hat{r} = 0$, the Maclaurin series gives

$$\lim_{\hat{r}\to 0}\frac{1}{\hat{r}}\frac{\partial\hat{C}}{\partial\hat{r}}(\hat{r}, \hat{t}) = \frac{\partial^2\hat{C}}{\partial\hat{r}^2}(0, \hat{t})$$

and then Eq. (39) at $\hat{r} = 0$ becomes

$$\frac{\partial\hat{C}}{\partial\hat{t}} = 3A_1\frac{\partial^2\hat{C}}{\partial\hat{r}^2} \tag{43}$$

The difference form of this equation is

$$\frac{\hat{C}_{0,j+1} - \hat{C}_{0,j}}{\Delta\hat{t}} = 3A_1\left(\frac{\hat{C}_{1,j} - 2\hat{C}_{0,j} + \hat{C}_{-1,j}}{(\Delta\hat{r})^2}\right) \tag{44}$$

Table 1 Cathode model parameters used in the numerical simulations

Name	Symbol	Value	Reference
Young's modulus	E	370.0 GPa	[1]
Poisson's ratio	ν	0.20	[1]
Li stoichiometric concentration	$C_{100\%}$	25.72 kmol m^{-3}	[40]
Gas constant	R	8.314 J mol^{-1} K^{-1}	—
Temperature	T	293 K	—
Linear chemical-expansion coefficient	$\hat{\beta}_L$	$-0.5417\Delta\hat{C} + 2.2072$	(Current study)
Constant chemical-expansion coefficient	$\hat{\beta}_C$	1.2101	(Current study)
Dimensionless compositional range	Δx	0.18	[28]

Furthermore, from $(\partial\hat{C}/\partial\hat{r})(0,\hat{t}) = 0, \hat{C}_{-1,j} = \hat{C}_{1,j}$. Thus, Eq. (44) reduces to

$$\hat{C}_{0,j+1} = \hat{C}_{1,j}(6A_1 s) + \hat{C}_{0,j}(1 - 6A_1 s)$$

The parameters used in the numerical simulations are summarized in Table 1.

8 Computational Results

The intent of this investigation is to ascertain the importance of including a variable chemical-expansion coefficient, $\beta(C)$, in the analysis of the nonlinear volumetric changes experienced by LIB cathodes during lithiation or delithiation. Both linear β (β_L) and constant β (β_C) are considered. In dimensionless form, these are

$$\hat{\beta}_L = \hat{\xi}\Delta\hat{C} + \hat{\eta} \quad \text{and} \quad \hat{\beta}_C = \hat{\eta}$$

The case $\hat{\beta} = 0$ is also considered; this is to demarcate the significance of incorporating the mechanical contribution in the Fickian relation. In order to delineate the nature of the coupled relation of SID and DIS, three cases are considered: (i) fictitious choices for the parameters $\hat{\eta}$ and $\hat{\xi}$; (ii) no stress-assisted diffusion (classical Fick's law, $\hat{\beta} = 0$); and (iii) experimental $\hat{\beta}$ parameters for contracting/expanding Li_xCoO_2, based on published data [28]. In (iii), the data are approximated by both $\hat{\beta}_C$ and $\hat{\beta}_L$. The $\hat{\beta}_L$-based simulations are oriented to the nonlinear volumetric strain that the material undergoes in the $0.37 \le x \le 0.55$ compositional range. Here, it is discussed if the impact of a linear-concentration-dependent $\hat{\beta}$ in the chemo-elastic response of the cathode material is significant.

8.1 Effect of β on SID. The effect of changing the parameters in $\hat{\beta}_L$ on Li-saturation time, $\hat{t}_s$ (saturation at $\hat{r} = 0.5$), is depicted in Fig. 2.[4] As $\hat{\xi}$ increases in positive values, with a fixed $\hat{\eta} = 1.0$, $\hat{t}_s$ declines dramatically.[5] As shown in Fig. 2(*a*), $\hat{t}_s$ deviates up to a 21% increment ($\hat{\xi} = -4$) or 45% decrement ($\hat{\xi} = 10$) from the constant-$\hat{\beta}_C$ assumption under the presented hypothetical case scenarios, depending on the nature of the nonlinear volumetric strain.

In Fig. 2(*b*), a concavelike response is described by the parameter $\hat{\eta}$, at a fixed value of $\hat{\xi} = 1.0$, suggesting that as $\hat{\eta} \approx 0$ it takes more time for maximum lithiation to occur. However, the varying $\hat{\eta}$ indicates that pronounced rises or decays in the volumetric change versus composition will conduct faster saturation in the material. Results demonstrate that the diffusion of Li is highly sensitive to minute changes in the definition of the nature of β; this preliminary assessment agrees with the work presented in Refs. [17] and [14], where a strong effect of a constant Ω on Li concentration (and stress–strain profile) in the $Li_xMn_2O_4$ material was elucidated upon various Ω-case scenarios. Findings show that the chemo-elastic response of the material is strongly β-dependent.

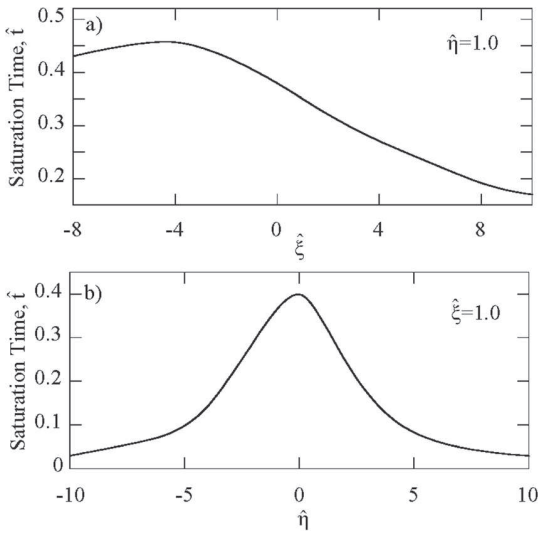

Fig. 2 Influence of hypothetical parameters of a linear $\hat{\beta}$ on saturation time, $\hat{t}_s$, within the Li_xCoO_2 cathode particle ($0.37 \le x \le 0.55$) at $\hat{r} = 0.5$: (*a*) $\hat{\xi}$ effect at fixed $\hat{\eta} = 1.0$ and (*b*) $\hat{\eta}$ effect at fixed $\hat{\xi} = 1.0$ during potentiostatic discharge conditions

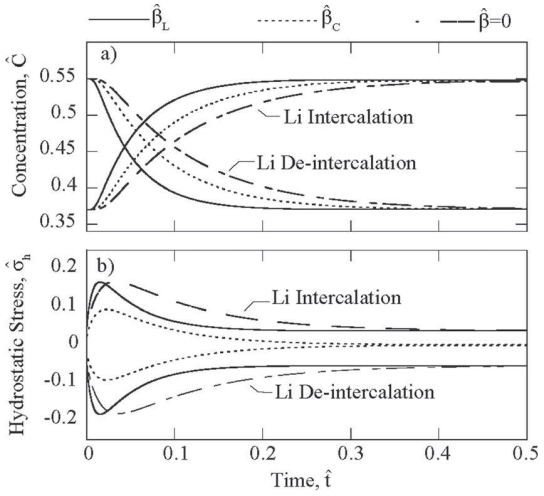

Fig. 3 Influence of the $\hat{\beta}$ parameter at $\hat{r} = 0.5$ for normalized values on the (*a*) Li diffusion and (*b*) hydrostatic stress during discharge-and-charge potentiostatic conditions ($0.37 \le x \le 0.55$)

8.2 Effect of β on the Chemo-Elastic Response. For the remainder of this section, the parameter values used in $\hat{\beta}_C$ and $\hat{\beta}_L$

[4]For practical purposes, the saturation time is considered to be the time needed to lithiate the cathode particle until it reaches the maximum concentration of the compositional range studied (i.e., Li0.55CoO2).

[5]Note that the terms $\hat{C}$ and x in LixCoO2 are equivalent.

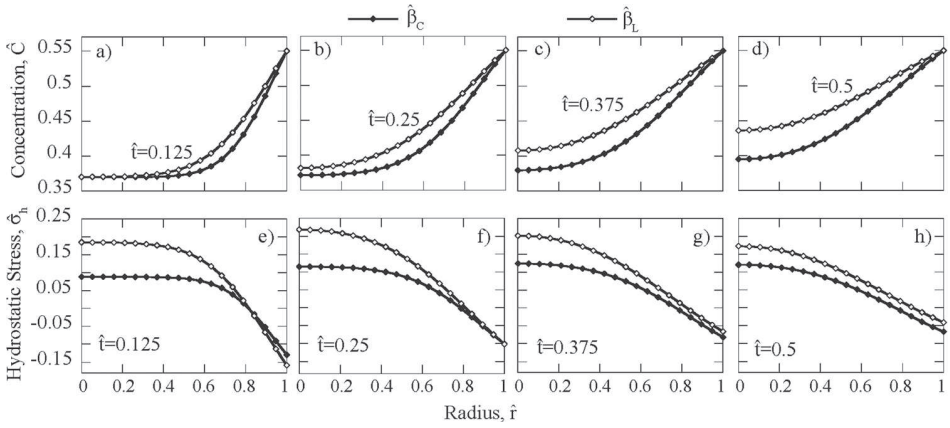

Fig. 4 Evolution of the Li concentration profile across the Li_xCoO_2 particle radius (*a*)–(*d*) and hydrostatic stress (*e*)–(*f*) under discharge potentiostatic conditions ($0.37 \le x \le 0.55$). Note that no steady state is reached by the reported $\hat{t}$.

are found in Table 1. Note that the values of $\hat{\xi}$ and $\hat{\eta}$ presented correspond to the volumetric strain of Li_xCoO_2 in the compositional range selected.

Defining the coupled dependence of the relation of SID and DIS is rather complex due to the reciprocate contribution of the stress–strain state and the Li-composition in chemo-elastic behavior of the electrode particle. This is because each chemo-elastic parameter controls the degree of influence that the hydrostatic-stress gradient has on Li migration and vice-versa. Both chemo-elastic processes, DIS and SID, are originated from the nonuniform nature of composition gradients and stress gradients, respectively. While the former develops self stresses in unconstrained electrode particles, the latter affects the rate of the pre-existing diffusion process. Figure 3(*a*) shows that both lithiation and delithiation are accelerated under a linear chemical-expansion coefficient, $\hat{\beta}_L$, followed by the constant $\hat{\beta}_C$-based concentration and the stress-independent Li-diffusion ($\hat{\beta} = 0$ case), in that order. This indicates that the hydrostatic-stress gradients, $\nabla\sigma_h$, that develop in the particle noticeably assist either electrochemical process that the cathode material undergoes. For instance, at $\hat{t} = 0.1$, the concentration of Li that results from the mechanical contribution with a linear $\hat{\beta}_L$, is nearly 6% higher with respect to contributions accounting for the $\hat{\beta}_C$ effect, and up to 11% greater when no mechanical influence is taken into account under the $\hat{\beta} = 0$ case (i.e., based on the classical Fickian relation). The difference among the various concentration fields studied through $\hat{t}$ is more accentuated during the first 20% of the lithiation process ($\hat{t} = 0.2$).[6] It is found that the concentration gradients, ∇C, in coupled cases are lesser in value with respect to those corresponding to the uncoupled model. This indicates that stress generated upon ∇C results in a driving force by which the migration of Li into/out the inner layers of the particle is promoted during both intercalation and deintercalation. Hence, stress-coupling aids the diffusion phenomena significantly.

According to Fig. 3(*b*), the hydrostatic stress difference between $\hat{\beta}_L$ and $\hat{\beta}_C$ is on the order of 46%. A similar observation is found in Ref. [41] for a $Li_xMn_2O_4$ numerical model suggesting electrode fracture proneness. Christensen and Newman [41] reported radial stresses of up to 31% greater for fictitious linear Ω cases with respect to constant Ω, depending on the steepness of the lattice-constant slope as a function of Li content. Note that $\hat{\sigma}_h$ in the decoupled flux case scenario has been defined based on the $\hat{\beta}_L$ concept and, subsequently, the peaks of hydrostatic stresses in the linear-$\hat{\beta}_L$ case and the stress-independent flux case are of equal magnitude, see Eq. (32). However, the corresponding response of $\hat{\beta}_L$ and $\hat{\beta}_C$ simulations the does not coincide along $\hat{r}$; the $\hat{\sigma}_h$ peaks are found at $\hat{r} = 0.02$ for the $\hat{\beta}_L$ (and $\hat{\beta}_C$) and at $\hat{r} = 0.03$ for the $\hat{\beta} = 0$ case, respectively. At $\hat{t} = 0.5$, $\hat{\sigma}_h$ is on the order of 0.03 for both the linear- and zero-$\hat{\beta}$ cases under the lithiation process and $\hat{\sigma}_h = -0.05$ under the delithiation condition. In both electrochemical processes, this is $\hat{\sigma}_h = 0.00$ under the constant-$\hat{\beta}_C$ assumption. The latter infers the $\sigma_{rr} = \sigma_{\theta\theta}$ relation is reached midway of the Li intercalation or deintercalation when the volumetric strain of the material varies linearly with composition. Note this is shown later in Sec. 8.3; it is important to notice that the particle is not under steady-state conditions at $\hat{t} = 0.5$.

During both the discharge and charge of the cathode, the Li diffusion occurs at a more sluggish fashion when $\hat{\beta} = 0$, leading to a more nonuniform composition field. This is because the mechanical contribution in the flux relation is absent and, therefore, unaffected concentration gradients become dominant. As a consequence, mechanical strains rise in a more heterogeneous fashion and prevail in time throughout the remainder of the intercalation (internal tensile $\hat{\sigma}_h$) and deintercalation (internal compressive $\hat{\sigma}_h$) processes. It can be established that the degree at which the linear-concentration-dependent β affects the DIS is much greater than the influence this chemical parameter has on the assisted diffusion, SID.

8.3 Effect of β on DIS and SID. The analysis presented in this section is intended to discern the linear versus constant composition-relation effect of the chemical-expansion coefficient. For this, both electrochemical processes are simulated and results are summarized in Figs. 4 and 5 for the intercalation- and deintercalation condition, respectively. In Figs. 4(*a*)–4(*d*) it is observed that the Li-concentration profile under the $\hat{\beta}_C$-lithiation assumption is relatively steady through $\hat{t}$, comparing to the $\hat{\beta}_L$ case, particularly at $\hat{r} \approx 0.0$. In Figs. 4(*e*)–4(*h*) it is evident that during the intercalation process, $\hat{\sigma}_h$ on the surface of the particle (which equals to $\sigma_{\theta\theta}$) becomes compressive in nature whereas in the center of the sphere, tensile stresses rise. This is due to the contraction that the Li_xCoO_2 cathode material undergoes during the discharge process. Similar Li-diffusion and stress response was obtained for the delithiation process simulations, see Figs. 5(*a*)–5(*h*), where compressive $\hat{\sigma}_h$ rises on the surface whereas the inside of the particle remains in tension. It is found that, in a correlation fashion, both $\hat{\beta}_L$ and $\hat{\beta}_C$ influence $\nabla\hat{\sigma}_h$ and $\nabla\hat{C}$. Hence, the β parameter constitutes a key parameter in defining the degree of (a) the driving forces in the diffusion of Li and (b) the stress–strain response of the particle.

Figures 4(*a*)–4(*e*) and 5(*a*)–5(*e*) show that during the onset of the electrochemical intercalation and deintercalation ($\hat{t} = 0.125$), the inner layers of the particle experience no diffusion and the

[6]Maximum discharge (at $\hat{C} = 0.55$) or charge (at $\hat{C} = 0.37$) is reached at $\hat{t} = 0.5$.

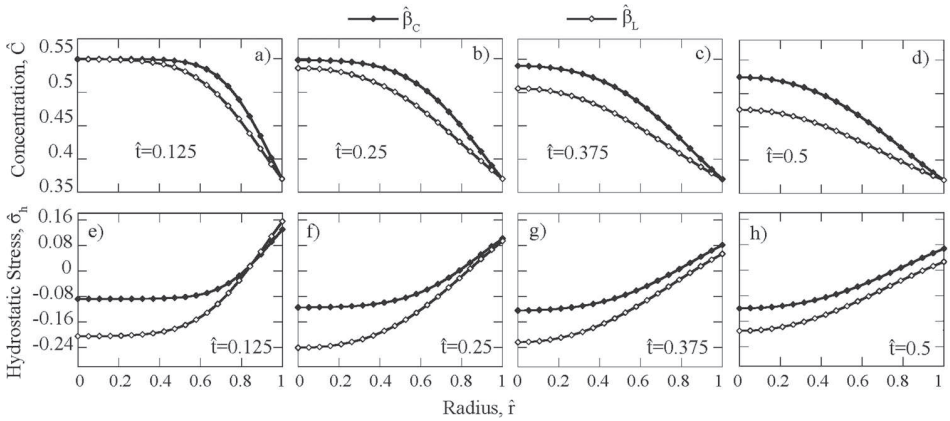

Fig. 5 Evolution of the Li concentration profile across the Li_xCoO_2 particle radius (*a*)–(*d*) and hydrostatic stress (*e*)–(*f*) under charge potentiostatic conditions ($0.55 \geq x \geq 0.37$). Note that no steady state is reached by the reported $\hat{t}$.

stress is uniformly distributed, as could be anticipated. The correlation of SID and DIS at this state is then established; this is $\nabla\hat{C} \approx 0$ and $\nabla\hat{\sigma}_h \approx 0$; the latter is particularly more pronounced with $\hat{\beta}_C$ as the condition extends through time ($\hat{t} = 0.25$). Figures 4 and 5 demonstrate that the stress evolution always facilitates the diffusion of Li into or out of the interior of the Li_xCoO_2 cathode material. More explicitly, this suggests the absolute value in the right-hand side of Eq. (29) prevails, i.e., $\nabla\hat{\sigma}_h < 0$ and $\nabla\hat{C} > 0$ during intercalation, and $\nabla\hat{\sigma}_h > 0$ and $\nabla\hat{C} < 0$ during intercalation. The reciprocate effects of the resulting chemo-elastic parameter gradients, $\nabla\hat{\sigma}_h$ and $\nabla\hat{C}$, are greater than that of the hydrostatic stress, $\hat{\sigma}_h$, alone.

9 Conclusions

The purpose of this work is to provide an insight on the role of the composition-dependent chemical-coefficient expansion in the chemo-elastic response of the Li_xCoO_2 cathode material. A new formulation for the SID and DIS that emerge during electrochemical processes is developed and simulated in this study. This is based on a modified nonlocal Fickian relation using an ideal spherical particle under potentiostatic control.

Findings show that the reciprocate relation of SID and DIS is highly sensitive to the chemical-coefficient expansion β. The linear β_L case study results in a 11% higher diffusion of Li with respect to the stress-decoupling case ($\beta = 0$) and 6% respecting the typical constant chemical-expansion coefficient, β_C. Likewise, at the end of the lithiation process, the radial stresses as diffusion progresses yield a difference of 39% more compressive stresses (on the particle surface) and 49% more tensile stresses (in the particle core), between the $\beta = 0$ and β_C cases, predicting more deleterious stresses for the stress-decoupling case. This is due to the faster diffusion that is induced by the linear-β_L case, which in turn results in less inhomogeneous concentration fields. It was evidenced that mechanical contribution in diffusion-stress-coupling relation has a greater effect on the chemical field (i.e., the influence of the linear β_L on the SID becomes dominant) than in the elastic field (in terms of hydrostatic stresses). It is found that the internal hydrostatic-stress gradients significantly enhance diffusion during Li intercalation/deintercalation under the linear-β_L formulation in the Li_xCoO_2 material. This suggests that the stress decoupling in the Fickian-based relation could mispredict the chemo-stress–strain response of the LIB electrode, and the linear-β_L model constitutes a key parameter in demarcating the chemo-elastic coupled phenomena.

It was determined that the effect of a linear-β_L, which is Li-content-dependent, is not of a negligible nature. The linearity described by this chemical parameter under the conditions examined facilitates in a greater fashion the diffusion of Li during its insertion and extraction. As a comparison to scenarios wherein this parameter is defined as a constant (β_C), the emanating internal compressive hydrostatic stresses (or internal tensile stresses under deintercalation) that can develop upon the relation of SID and DIS are 46% higher under the linear-β_L model. From the mechanical perspective, the integrity of the cathode material can be compromised during the nonlinear volumetric changes that the Li_xCoO_2 cathode material withstands since DIS are greater in magnitude when the linear-β_L concept is imposed.

Acknowledgment

This work was supported by the Office of Naval Research via Grant No. N00014-08-1-0539 to the Colorado School of Mines.

References

[1] Malavé, V., Berger, J. R., Zhu, H., and Kee, R. J., 2014, "A Computational Model of the Mechanical Behavior Within Reconstructed Li_xCoO_2 Li-Ion Battery Cathode Particles," Electrochim. Acta, **130**, pp. 707–717.

[2] Larché, F. C., and Cahn, J. W., 1985, "The Interactions of Composition and Stress in Crystalline Solids," Acta Metall., **33**(3), pp. 331–357.

[3] Bohn, E., Eckl, T., Kamlah, M., and McMeeking, R., 2013, "A Model for Lithium Diffusion and Stress Generation in an Intercalation Storage Particle With Phase Change," J. Electrochem. Soc., **160**(10), pp. A1638–A1652.

[4] Qi, Y., Guo, H., Hector, L. G., and Timmons, A., 2010, "Threefold Increase in the Young's Modulus of Graphite Negative Electrode During Lithium Intercalation," J. Electrochem. Soc., **157**(5), pp. A558–A566.

[5] Deshpande, R., Qi, Y., and Cheng, Y.-T., 2010, "Effects of Concentration-Dependent Elastic Modulus on Diffusion-Induced Stresses for Battery Applications," J. Electrochem. Soc., **157**(8), pp. A967–A971.

[6] Shenoy, V. B., Johari, P., and Qi, Y., 2010, "Elastic Softening of Amorphous and Crystalline Li-Si Phases With Increasing Li Concentration: A First-Principles Study," J. Power Sources, **195**(19), pp. 6825–6830.

[7] Gao, Y. F., and Zhou, M., 2011, "Strong Stress-Enhanced Diffusion in Amorphous Lithium Alloy Nanowire Electrodes," J. Appl. Phys., **109**(1), p. 014310.

[8] Yang, B., He, Y.-P., Irsa, J., Lundgren, C. A., Ratchford, J. B., and Zhao, Y.-P., 2012, "Effects of Composition-Dependent Modulus, Finite Concentration and Boundary Constraint on Li-Ion Diffusion and Stresses in a Bilayer Cu-Coated Si Nano-Anode," J. Power Sources, **204**, pp. 168–176.

[9] Stournara, M. E., Guduru, P. R., and Shenoy, V. B., 2012, "Elastic Behavior of Crystalline Li-Sn Phases With Increasing Li Concentration," J. Power Sources, **208**, pp. 165–169.

[10] He, Y.-L., Hu, H. J., Song, Y.-C., Guo, Z.-S., Liu, C., and Zhang, J.-Q., 2014, "Effects of Concentration-Dependent Elastic Modulus on the Diffusion of Lithium Ions and Diffusion Induced Stress in Layered Battery Electrodes," J. Power Sources, **248**, pp. 517–523.

[11] Lantelme, F., Groult, H., and Kumagai, N., 2000, "Study of the Concentration-Dependent Diffusion in Lithium Batteries," Electrochim. Acta, **45**(19), pp. 3171–3180.

[12] Renganathan, S., and White, R. E., 2011, "Semianalytical Method of Solution for Solid Phase Diffusion in Lithium Ion Battery Electrodes: Variable Diffusion Coefficient," J. Power Sources, **196**(1), pp. 442–448.

[13] Crank, J., 1975, *The Mathematics of Diffusion*, Oxford University, New York.

[14] Purkayastha, R. T., and McMeeking, R. M., 2012, "An Integrated 2-D Model of a Lithium Ion Battery: The Effect of Material Parameters and Morphology on Storage Particle Stress," Comput. Mech., **50**(2), pp. 209–227.
[15] Darling, R., and Newman, J., 1998, "Diffusion in $Li_yMn_2O_4$," 193rd Meeting of the Electrochemical Society, San Diego, CA, May 3–8, Vol. 98–10, pp. 1–13.
[16] Darling, R., and Newman, J., 1999, "Dynamic Monte Carlo Simulations of Diffusion in $Li_yMn_2O_4$," J. Electrochem. Soc., **146**(10), pp. 3765–3772.
[17] Purkayastha, R., and McMeeking, R. M., 2012, "A Linearized Model for Lithium Ion Batteries and Maps for Their Performance and Failure," ASME J. Appl. Mech., **79**(3), p. 031021.
[18] Garcia, R. E., Chiang, Y.-M., Carter, W. C., Limthongkul, P., and Bishop, C. M., 2005, "Microstructural Modeling and Design of Rechargeable Lithium-Ion Batteries," J. Electrochem. Soc., **152**(1), pp. A255–A263.
[19] Zhang, X., Shyy, W., and Sastry, A. M., 2007, "Numerical Simulation of Intercalation-Induced Stress in Li-Ion Battery Electrode Particles," J. Electrochem. Soc., **154**(10), pp. A910–A916.
[20] Zhang, X., Sastry, A. M., and Shyy, W., 2008, "Intercalation-Induced Stress and Heat Generation Within Single Lithium-Ion Battery Cathode Particles," J. Electrochem. Soc., **155**(7), pp. A542–A552.
[21] Woodford, W. H., Chiang, Y.-M., and Carter, W. C., 2010, "Electrochemical Shock of Intercalation Electrodes: A Fracture Mechanics Analysis," J. Electrochem. Soc., **157**(10), pp. A1052–A1059.
[22] Chung, D.-W., Balke, N., Kalinin, S. V., and Garcia, R. E., 2011, "Virtual Electrochemical Strain Microscopy of Polycrystalline $LiCoO_2$ Films," J. Electrochem. Soc., **158**(10), pp. A1083–A1089.
[23] Park, J., Lu, W., and Sastry, A. M., 2011, "Numerical Simulation of Stress Evolution in Lithium Manganese Dioxide Particles Due to Coupled Phase Transition and Intercalation," J. Electrochem. Soc., **158**(2), pp. A201–A206.
[24] Seo, J. H., Chung, M., Park, M., Han, S. W., Zhang, X., and Sastry, A. M., 2011, "Generation of Realistic Particle Structures and Simulations of Internal Stress: A Numerical/AFM Study of $LiMn_2O_4$ Particles," J. Electrochem. Soc., **158**(4), pp. A434–A442.
[25] Song, Y., Lu, B., Ji, X., and Zhang, J., 2012, "Diffusion Induced Stresses in Cylindrical Lithium-Ion Batteries: Analytical Solutions and Design Insights," J. Electrochem. Soc., **159**(12), pp. A2060–A2068.
[26] Lim, C., Yan, B., Yin, L., and Zhu, L., 2012, "Simulation of Diffusion-Induced Stress Using Reconstructed Electrodes Particle Structures Generated by Micro/Nano-CT," Electrochim. Acta, **75**, pp. 279–287.
[27] Yoshio, M., Brodd, R. J., and Kozawa, A., eds., 2010, *Lithium-Ion Batteries: Science and Technology*, Springer, New York.
[28] Reimers, J. N., and Dahn, J. R., 1992, "Electrochemical and In Situ X-Ray Diffraction Studies of Lithium Intercalation in Li_xCoO_2," J. Electrochem. Soc., **139**(8), pp. 2091–2097.
[29] Allen, J. L., Ding, M. S., Xu, K., Zhang, S., and Jow, T. R., 2004, "$Li_{1+x}Fe_{1-x}PO_4$: Electronically Conductive Lithium Iron Phospho-Olivines With Improved Electrochemical Performance," 205th Electrochemical Society Fall Meeting, Honolulu, HI, October 3–8, Vol. 28, pp. 198–204.
[30] Ohzuku, T., and Makimura, Y., 2006, "Formation of Solid Solution and Its Effect on Lithium Insertion Schemes for Advanced Lithium-Ion Batteries: X-Ray Absorption Spectroscopy and X-Ray Diffraction of $LiCoO_2$, $LiCo_{1/2}Ni_{1/2}O_2$, and $LiNiO_2$," Res. Chem. Intermed., **32**(5), pp. 507–521.
[31] Huggins, R. A., 2009, *Advanced Batteries: Materials Science Aspects*, Springer, New York.
[32] Wakihara, M., and Yamamoto, O., eds., 1998, *Lithium Ion Batteries: Fundamentals and Performance*, Wiley, Weinheim, Germany.
[33] Mal, A. K., and Singh, S. J., 1991, *Deformation of Elastic Solids*, Prentice-Hall, Englewood Cliffs, NJ.
[34] Yang, F., 2005, "Interaction Between Diffusion and Chemical Stresses," Mater. Sci. Eng. A, **409**(1–2), pp. 153–159.
[35] Cheng, Y.-T., and Verbrugge, M. W., 2009, "Evolution of Stress Within a Spherical Insertion Electrode Particle Under Potentiostatic and Galvanostatic Operation," J. Power Sources, **190**(2), pp. 453–460.
[36] Hao, F., Gao, X., and Fang, D., 2012, "Diffusion-Induced Stresses of Electrode Nanomaterials in Lithium-Ion Battery: The Effects of Surface Stress," J. Appl. Phys., **112**(10), p. 103507.
[37] Song, Y., Shao, X., Guo, Z., and Zhang, J., 2013, "Role of Material Properties and Mechanical Constraint on Stress-Assisted Diffusion in Plate Electrodes of Lithium Ion Batteries," J. Phys. D: Appl. Phys., **46**(10), p. 105307.
[38] Timoshenko, S., and Goodier, J. N., 1970, *Theory of Elasticity*, McGraw-Hill, New York.
[39] Smith, G. D., 1985, *Numerical Solution of Partial Differential Equations*, 3rd ed., Oxford University, Oxford, UK.
[40] Wiedemann, A. H., Goldin, G. M., Barnett, S. A., Zhu, H., and Kee, R. J., 2013, "Effects of Three-Dimensional Cathode Microstructure on the Performance of Lithium-Ion Battery Cathodes," Electrochim. Acta, **88**, pp. 580–588.
[41] Christensen, J., and Newman, J., 2006, "A Mathematical Model of Stress Generation and Fracture in Lithium Manganese Oxide," J. Electrochem. Soc., **153**(6), pp. A1019–A1030.